A chitosan–dipotassium orthophosphate hydrogel for the delivery of Doxorubicin in the treatment of osteosarcoma

Hang T. Ta [a], Crispin R. Dass [b],*, Ian Larson [c], Peter F.M. Choong [b,d], Dave E. Dunstan [a]

[a] Department of Chemical and Biomolecular Engineering, University of Melbourne, VIC 3010, Australia
[b] Departments of Orthopaedics and Surgery, St Vincent's Hospital Melbourne, Melbourne, VIC 3065, Australia
[c] Monash Institute of Pharmaceutical Sciences, Monash University, VIC 3052, Australia
[d] Sarcoma Service, Peter MacCallum Cancer Centre, VIC 3002, Australia

ARTICLE INFO

ABSTRACT

The current management of primary osteosarcoma (OS) and its secondary metastasis is limited by the lack of an efficient drug delivery system. Here we report an *in situ* gelling chitosan/dipotassium orthophosphate hydrogel system designed to directly deliver the frontline chemotherapeutic agent (Doxorubicin) in a sustained time period to tumor sites. A significant reduction of both primary and secondary OS in a clinically relevant orthotopic model was measured when doxorubicin was administered with the hydrogel. This hydrogel delivery system also reduced cardiac and dermal toxicity of Doxorubicin in mice. The results obtained from this study demonstrate the potential application of a biodegradable hydrogel technology as an anti-cancer drug delivery system for successful chemotherapy.

1. Introduction

Osteosarcoma (OS) is the most common type of malignant bone cancer, and the sixth most common type of cancer in children and young adults [1,2]. It also represents the second highest cause of cancer-related death in this age group [3]. OS begins in bones, frequently localizes in the distal femur and proximal tibia region, and usually metastasizes to the lungs or other bones. The overall survival rate of patients was 10% before the 1970s when treatment was mainly limb amputation [1]. The rate dramatically increased to approximately 60–70% once multi-agent chemotherapy followed by surgery has been introduced [4]. Currently, chemotherapy drugs are administered both before and after surgery. Despite significant effort in the field, no major changes in treatment and outcome have been achieved.

Contemporary chemotherapy for OS is normally the combination of different chemotherapeutic agents administered intravenously or orally [5,6]. However, most chemotherapeutics also carry the risk of both short-term and long-term toxic effects. Doxorubicin (Dox) for example, can cause nausea, vomiting, heart and skin complications. When the cumulative dose of Dox reaches 700 mg/m^2, the risks of developing cardiac side-effects dramatically increase [7]. Due to its high toxicity and hence narrow therapeutic index, increasing systemic dose to achieve desirable high concentration of drug at the tumor site is difficult. In addition, the concentration of systemically-administered drug at the bony cancerous site is likely to be very low because the bone is only a moderately-perfused organ [8]. It has been reported that only 0.52 μg of Dox accumulated in 1 g marrow after an intravenous administration of 30 mg/m^2 of Dox [9]. Therefore, a localized and targeted drug delivery system (DDS) is essential to overcome these problems in the treatment of OS.

Most of the studied Dox DDSs such as liposomes [10,11], microspheres [12], polymeric micelles [13,14] and conjugates [15] are usually administered intravenously, limiting the dosage for treatment of OS. Magnetic liposomes [16] and hydroxyapatite implants [17] have been developed and tested successfully in *in vivo* models of OS. However, these DDSs require the surgical insertion of magnets and implants at treatment sites, which reduces the comfort and convenience to patients. In this study, we developed a biodegradable and non-cytotoxic *in situ* gelling chitosan/dipotassium orthophosphate (Chi/DPO) hydrogel DDS for delivery of Dox in OS treatment. Different Chi/DPO formulations were characterized and the optimal formulation was selected. A clinically relevant orthotopic mice model of OS [3] was employed for the *in vivo* study.

* Corresponding author.
E-mail address: crispin.dass@svhm.org.au (C.R. Dass).

Table 1
Chi/DPO formulations for Dox delivery.

Formulation	Components					
	Low Mw chitosan solution			K_2HPO_4 solution		Doxorubicin[a]
	Concentration (%)	Heat-treating time (hours)	Volume (µl)	Concentration (%)	Volume (µl)	
Chi/DPO1–Dox	2	0	900	50	60	106.4 µl
Chi/DPO2–Dox	2.5	9	900	25	100	111.2 µl
Chi/DPO3–Dox	2.5	9	900	28	100	111.2 µl
Chi/DPO4–Dox	2.9	26	900	25	100	111.2 µl
Chi/DPO5–Dox	2.9	26	900	22	70	108.0 µl

[a] Doxorubicin stock solution is 25 mg/ml. Final concentration of Dox in formulations is 2.5 mg/ml Chi/DPO.

2. Materials and methods

2.1. Materials

Low molecular weight chitosan was obtained from Fluka BioChemika (Switzerland). Dipotassium phosphate (K_2HPO_4) (DPO) and acetic acid (CH_3COOH) were purchased from Ajax Finechem (Australia). Doxorubicin was obtained from Sigma–Aldrich, Australia. The human SaOS-2 OS cell line attained from the American Type Culture Collection (ATCC) was cultured in α-MEM (Invitrogen, Australia) supplemented with 10% fetal calf serum (FCS, Invitrogen, giving complete medium, CM) in a humidified 5% CO_2 atmosphere. Cells were used within 20 passages. A seeding cell population of exponentially-growing cells greater than 95% viability was used for all assays. Female 5-week-old Balb/c nude mice (Animal Resource Centre, Perth, Australia) were used for orthotopic injection of SaOS-2 cells. Mice were housed and maintained at the BioResources Centre (St Vincent's Hospital, Australia) as previous described [18]. All animal experimentations were approved by the St Vincent's Health Animal Ethics Committee.

2.2. Preparation of hydrogel solution

Low Mw chitosan solutions were prepared by dissolving chitosan flakes in 0.1 M acetic acid overnight at room temperature under constant stirring. The resultant solutions were then filtered through 100 µm pore sized filters and stored under refrigeration, at 4 °C. Chitosan solutions of different concentrations were heated at 85 °C for different numbers of hours to reduce their viscosity. DPO solutions were prepared with distilled water and stored at 4 °C. Appropriate amounts of cold DPO solution (4 °C) were added into cold chitosan solution (4 °C) and mixed manually at room temperature until homogeneous.

2.3. Rheology analysis

Rheological measurements were performed using a Carri-Med CSL^2 100 controlled stress rheometer with cone (4 cm diameter, 1.59° angle) and plate geometry. The temperature of the plate (0–100 °C) was controlled by a Peltier unit. For all measurements, approximately 1 ml of each freshly prepared sample was introduced onto the plate at 18 °C. Evaporation of sample was prevented by using a solvent trap in conjunction with silicon oil sealing. All the measurements were performed in oscillation mode at a fixed frequency of 1 Hz and a strain of 1%, which is well within the measured linear viscoelastic region. The temperature evolution of G′ and G″ moduli were measured with change in temperature at a rate of 1 °C/min. The time evolution of G′ and G″ were measured at constant temperature of 37 °C. The gelation temperature and the gelation time were taken as the temperature and the time at which G′ and G″ were equivalent in value [19–21].

2.4. In vitro release study

Appropriate amounts of doxorubicin were added to chitosan solutions and mixed thoroughly. After being kept cold at 4 °C, the resultant chitosan/Dox solution was mixed manually with an appropriate amount of cold DPO solution (4 °C) until homogeneous. Five different Chi/DPO–Dox formulations were prepared as detailed in Table 1.

20 µl of the resultant Chi/DPO solution containing Dox was pipetted into a 1.5 ml eppendorf tube which was incubated at 37 °C for 1 h at which temperature the solution gelled. The formed gels occupied the bottom of the tubes and exposed to the release buffer with the same surface area (∼19.6 mm²). 1 ml of PBS pH 7.4 (Sigma, Australia) was pipetted into each tube. Controls included tubes containing blank hydrogel. The tubes were then placed in a shaking incubator (Ratek, Australia) maintained at 37 °C and shaking at 100 rpm.

At predetermined time intervals, 900 µl of the release buffer was sampled and stored at −20 °C for further analysis. Subsequently, 900 µl of fresh buffer was added to the tubes in order to maintain the constant volume of the release medium. The amount of Dox released from the hydrogel formulations was measured using Carry Fluorescence Spectrophotometer (Varian, Australia) with excitation wavelength at

490 nm and emission wavelength at 593 nm. Briefly, a standard curve with fluorescence intensity plotted vs. Dox concentration was prepared and the amount of Dox released was determined based on this curve. The percentage cumulative release was calculated based on the total Dox content.

2.5. Proliferation/viability assay

2 µl of Chi/DPO3–Dox was pipetted into a 6-well plate. The plate was incubated at 37 °C for 15 min 2 ml of medium containing cells was pipetted into each well at 20,000, 40,000, 60,000, 80,000, and 100,000 cells/well. After 2 days of incubation at 37 °C/5% CO_2, cell viability in each well was measured using the Cell Titer Blue (CTB) (Promega, Melbourne, Australia) assay according to manufacturer instructions. The results were recorded using absorbance measurement with BioRad Model 680 Microplate Reader. The readings were taken at 570 nm with 600 nm as a reference wavelength.

2.6. Apoptosis assay

Glass coverslips (Sigma–Aldrich) (22 mm × 22 mm) were immersed in 70% ethanol for 5 min and then were put into a 6-well plate. The plate was unclosed and left in the biohood until all ethanol was evaporated. 2 µl of Chi/DPO3–Dox was pipetted into each well of the plate. The plate was incubated at 37 °C for 15 min to allow the gelation of this formulation. Subsequently, 2 ml of medium containing 100,000 cells was pipetted into each well. After 1 day of incubation at 37 °C/5% CO_2, the glass coverslips were processed using the DeadEnd™ Colorimetric TUNEL system (Promega, Australia).

2.7. In vivo efficacy study

Mice were anaesthetised with ketamine (100 mg/kg) and xylazine (10 mg/kg). 10 µl of 50% matrigel containing 20,000 of SaOS-2 cells was intratibially injected into each mouse as described previously [3,18,22]. 3 weeks later, mice were randomized into 11 groups with 5 mice per group and administered treatments. Details of these treatment groups are summarized in Table 2. Mice were monitored 3 times a week. At the termination of the study (12 days later), tumors were measured using digital calipers and mice legs were X-rayed [23]. Mice were sacrificed and heart, lungs, tumor, skin, and limbs were removed and fixed in 4% paraformaldehyde. After rinsing with PBS, number of lung macrometastases was counted. All tissues were embedded in paraffin for histological analysis.

2.8. Histology

The limbs were decalcified and all tissues were embedded in paraffin for histological analysis according to standard conditions [24]. All tissues were sectioned at 4 µm and stained with hematoxylin and eosin as before. Sections were observed with a Nikon Eclipse TE2000-U microscope (Nikon, Australia) and photographed with SPOT Advanced software (SciTech, USA).

Table 2
Mice treatment cohorts.

Group	Injection per mouse	Site of injection
No treatment	100 µl of 0.9% normal saline	Intraperitoneal
Chi/DPO3	2 × 20 µl of blank Chi/DPO	Two opposite sites in the tibia muscle next to the tumor (peritumoral)
Dox	100 µl of Dox solution in 0.9% normal saline at 5 mg Dox/kg mouse	Intraperitoneal
Chi/DPO3–Dox	2 × 20 µl of Chi/DPO3–Dox at 5 mg Dox/kg mouse	Peritumoral

Table 3
Properties of Chi/DPO formulations.

Formulation	Gelation temperature (°C)	Gelation time at 20 °C (min)	Gelation time at 37 °C (min)	G′ at 37 °C (Pa)	pH at 20 °C
Chi/DPO1	28.2	7.1	Immediate	258.7	7.51
Chi/DPO2	27.2	5.9	Immediate	549.3	7.46
Chi/DPO3	25.4	3.4	Immediate	651.7	7.49
Chi/DPO4	22	1.0	Immediate	2701	7.54
Chi/DPO5	30.3	3.0	Immediate	1238	7.20

2.9. Statistical analysis

Data were analyzed for statistical significant using Student's t-test (2-tailed). A P-value ≤ 0.05 was considered significant.

3. Results

3.1. Characterization of Chi/DPO solutions

Five different Chi/DPO formulations were characterized and tested in an *in vitro* release study to figure out a suitable formulation for delivering Dox. They were prepared by varying chitosan concentration, orthophosphate concentration and drug loading parameters (Table 1).

Rheological characterization of these five formulations was performed to define their gelation temperatures, gelation time at both room temperature (20 °C) and physiological temperature (37 °C), and the gel strength at 37 °C. The pH of each formulation was also determined. The results are summarized in Table 3.

The *in vitro* release of the active ingredient Dox from these five formulations was studied over a period of 19 days. It was found that Chi/DPO hydrogels released Dox in a sustained manner over this period (Fig. 1A). Details of the initial burst effect, the gelation rate and the cumulative release percentage after 19 days for each formulation are summarized in Table 4.

Based on the pH, the gelation temperature, the gelation time at room temperature and at 37 °C, the initial burst and the *in vitro* release rate, Chi/DPO3 emerged as the suitable system for delivering Dox. To avoid complication, the pH of Chi/DPO needs to be around physiological pH (7.4). Furthermore, the Chi/DPO solution should gel in a reasonable time. The system must remain liquid to allow injection and must gel rapidly enough to prevent abundant drug leaking from an incompletely-formed hydrogel. In addition, the hydrogel matrix should release drugs or active therapeutic agents in a sustained manner with a low initial burst effect. Although Chi/DPO1 and Chi/DPO3 produced the same initial burst effect and Chi/DPO1 was more stable than Chi/DPO3 at room temperature, Chi/DPO3 was selected due to its relatively quicker release rate during linear phase (Table 4) and its easier syringeability.

The effect of Dox loading on its release pattern was also investigated by comparing release profiles of Chi/DPO3 formulations containing 2.5 and 0.5 mg Dox/ml hydrogel solution. The formulation with higher load exhibited a lower initial burst effect and slower release rate in terms of percentage (Fig. 1B). However, in terms of mass amount, it produced a higher initial burst (7 μg vs. 3 μg) within 1 day and a greater release rate (197 ng/day vs. 68 ng/day during linear stage) (Fig. 1C). These results complied with Fick's
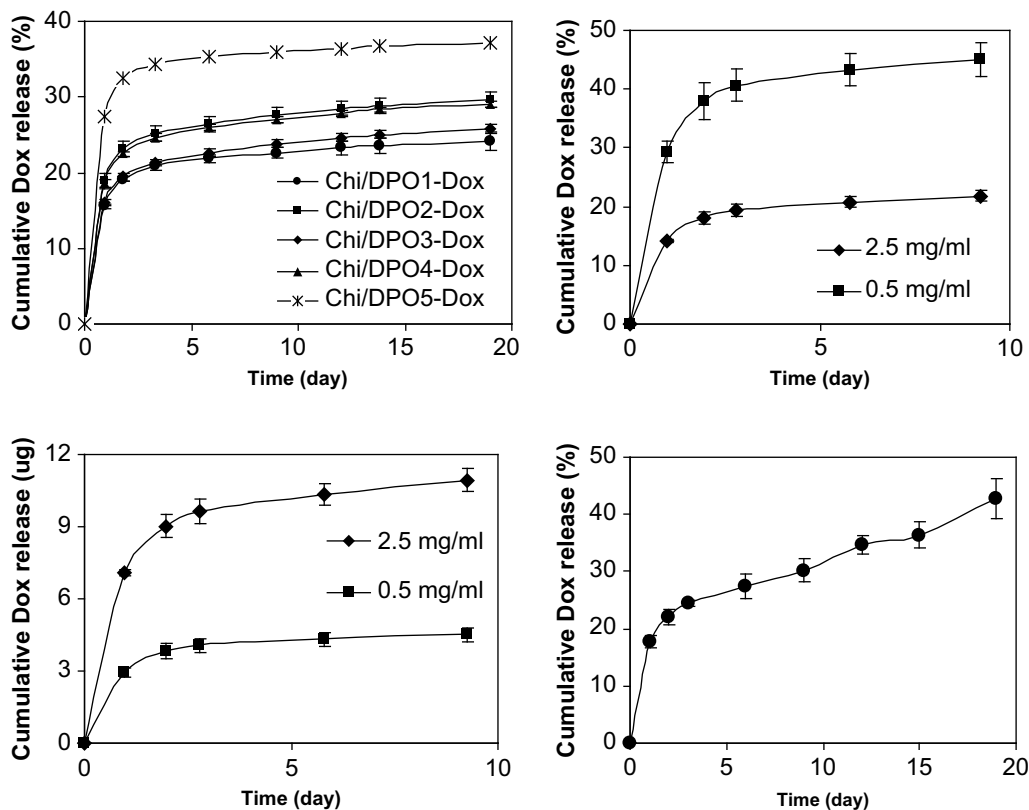

Fig. 1. *In vitro* release of Doxorubicin from different Chi/DPO formulations in PBS (pH 7.2) at 37 °C. (A) Formulations containing the same Dox loadings (2.5 mg Dox/ml Chi/DPO). Plots in terms of cumulative percentage of released protein. (■) Chi/DPO1–Dox, (▲) Chi/DPO2–Dox, (▼) Chi/DPO3–Dox, (◆) Chi/DPO4–Dox, (●) Chi/DPO5–Dox. (B) Formulations containing different Dox loadings. Plots in terms of cumulative percentage of released protein. (●) 2.5 mg Dox/ml Chi/DPO3, (▲) 0.5 mg Dox/ml Chi/DPO3. (C) Formulations containing different Dox loadings. Plots in terms of cumulative amount of released protein. (●) 2.5 mg Dox/ml Chi/DPO3, (▲) 0.5 mg Dox/ml Chi/DPO3. (D) *In vitro* release of Doxorubicin from Chi/DPO3 formulation in PBS (pH 7.2) containing lysozyme (8 μg/ml) at 37 °C. Plots in terms of cumulative percentage of released protein.

Table 4
Release characteristics of Chi/DPO–Dox formulations in PBS (pH 7.2).

Formulation	Initial burst release after 1 day (%)	Cumulative release after 19 days (%)	Release rate in linear phase (%/day)
Chi/DPO1–Dox	15.55 ± 0.22	24.09 ± 1.05	0.145 ± 0.129
Chi/DPO2–Dox	18.91 ± 1.08	29.58 ± 1.05	0.203 ± 0.147
Chi/DPO3–Dox	15.99 ± 0.46	25.84 ± 0.48	0.205 ± 0.068
Chi/DPO4–Dox	18.61 ± 0.45	29.02 ± 0.35	0.201 ± 0.046
Chi/DPO5–Dox	27.49 ± 0.14	37.15 ± 0.85	0.115 ± 0.110

diffusion that the driving force of diffusion is generated by the concentration gradient [25]. As the loading increased, the concentration gradient increased, thus dm or m (mass amount of Dox diffused or released) increased. The higher-loaded Chi/DPO3 formulation was used for the later experiments (discussed later).

The *in vitro* release of Chi/DPO3–Dox in PBS buffer containing lysozyme was also performed and is presented in Fig. 1D. In the presence of the enzyme, the initial burst was slightly affected and increased to 17.83 ± 1.05% (approximately 2% higher than the initial

burst in the absence of lysozyme). However, the release rate after the initial burst was 1.182 ± 0.312%/day which is nearly 6-fold higher than the rate in the absence of lysozyme (0.205 ± 0.068%/ day). These results indicate the more sustained release of Dox from Chi/DPO3 in the buffer containing lysozyme due to the degradation of the hydrogel matrix.

3.2. Therapeutic activities of Dox released from Chi/DPO3 hydrogel

SaOS-2, a human OS cell line, was employed to investigate the *in vitro* activities of both Dox released from Chi/DPO3 hydrogel matrix. We found that Chi/DPO3–Dox dramatically inhibited the proliferation of SaOS-2 cells (Fig. 2). Apoptosis, the major cause of cell death, was significantly enhanced in the presence of Chi/DPO3–Dox (Fig. 3), which helps to define the mechanism behind the decreased proliferation of SaOS-2 cells. Apoptosis was about 5-fold higher when Dox was incorporated into the chitosan hydrogel. These findings demonstrate the release of Dox from
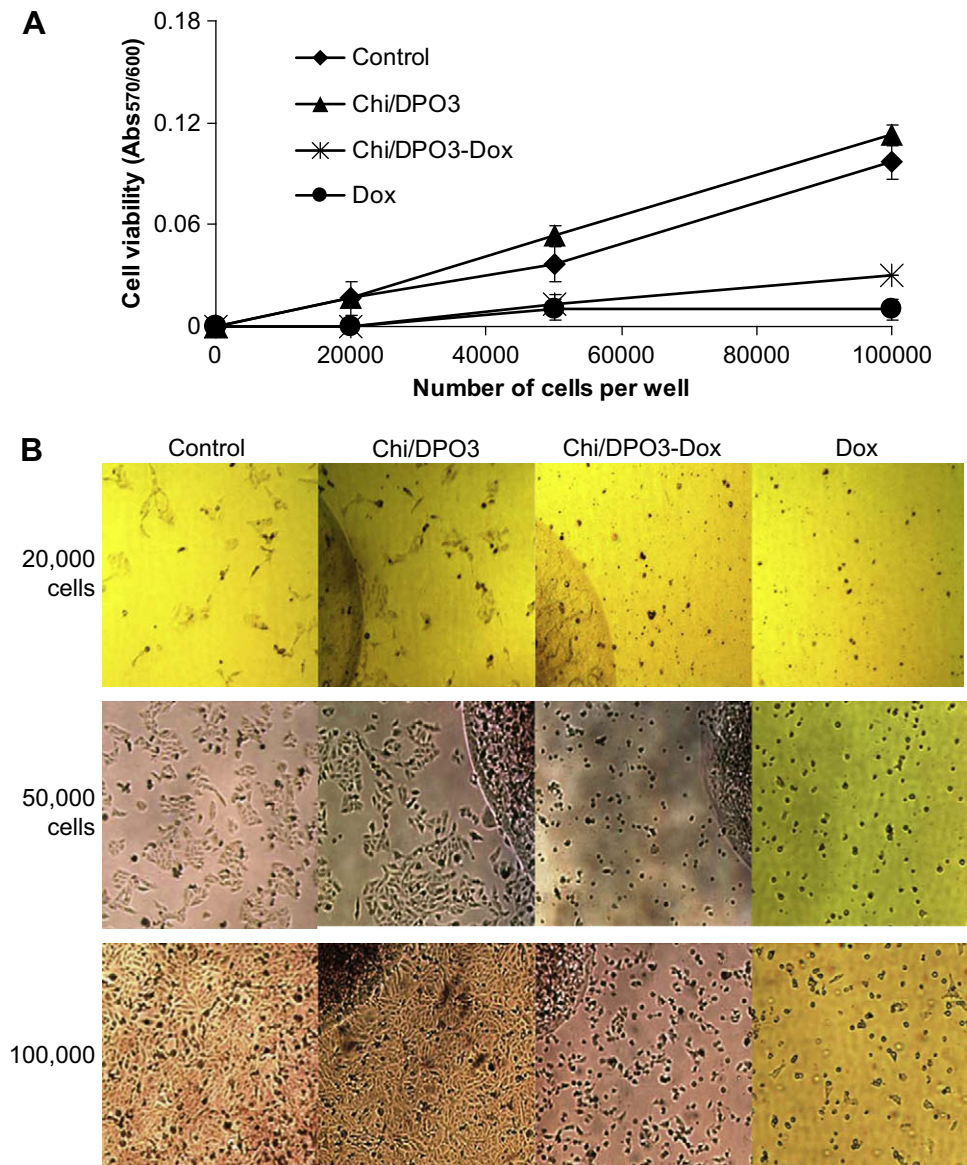

Fig. 2. Proliferation assay. (A) Proliferation assay results graph. (B) Images of SaOS-2 cell proliferation after 2 days of incubation. 2 μl of Chi/DPO3 or Chi/DPO3–Dox (2.5 mg Dox/ml Chi/DPO3) was used per well. Brown spherical shapes are blocks of hydrogels in wells.
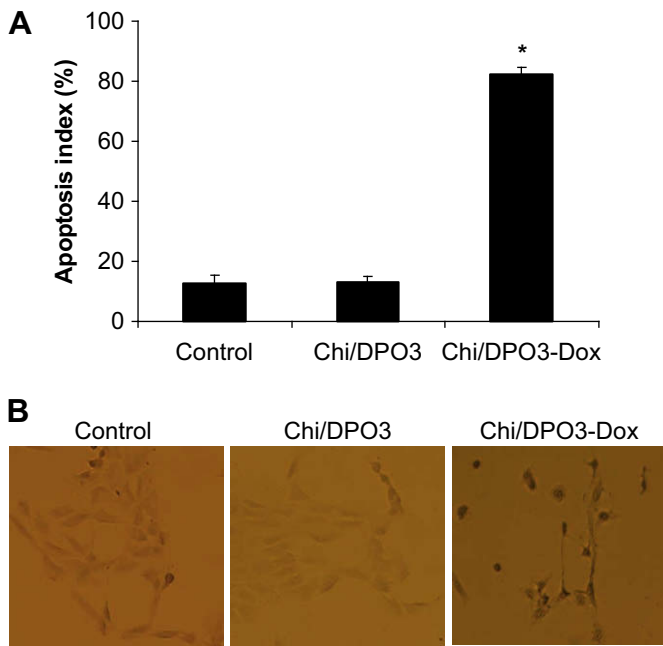
Fig. 3. Apoptosis assay. (A) Apoptosis assay results graph. (B) Images of apoptosis of SaOS-2 cells after 1 day of incubation. Apoptotic cells were TUNEL-stained showing a dark brown color. 2 μl of Chi/DPO3 or Chi/DPO3–Dox (2.5 mg Dox/ml CODS3) was used per well. *$P < 0.005$ vs. control group.

Chi/DPO3 to cells and demonstrated the preserved toxicity of the released Dox.

3.3. In vivo efficacy study

3.3.1. In vivo inhibition of primary tumor growth

Fig. 4 reveals the ability of Chi/DPO3–Dox to inhibit primary tumor growth at the tibia site. Chi/DPO3–Dox reduced the tumor volumes by approximately 50% compared to untreated (control) groups (Fig. 4A and C). Histological analysis of tumor tissues demonstrated that Chi/DPO3–Dox induced the highest level of cell apoptosis (37%) while free Dox and Chi/DPO3 induced less than 15% apoptosis (Fig. 4B and D). X-ray images revealed lesser evidence of bone degradation (osteolysis) in the groups of Chi/DPO3–Dox (Fig. 4E). Histology analysis also confirmed less osteolysis in this treatment group while significant osteolysis occurred in the other cohorts of mice (Fig. 4F).

3.3.2. In vivo inhibition of secondary tumor growth

In addition to the activity of Chi/DPO3–Dox at the primary bone tumor site, its activity at the secondary tumor site was also observed. The number of pulmonary (lung) metastases decreased approximately 1.5-fold in the Chi/DPO3–Dox group (Fig. 5A), compared to those in the other groups. Histological examination of dissected lungs also revealed smaller metastases in the Chi/DPO3–Dox group (Fig. 5B).

3.3.3. Reduced systemic side-effects of Dox released from Chi/DPO3 hydrogel

We found that controlled and sustained release of Dox via Chi/DPO3 considerably reduced its side-effects in mice including cardiotoxicity (Fig. 6A) and skin toxicity (Fig. 6B). Histology of heart sections showed cytoplasmic vacuolization (Fig. 6A3) and vascular dilation (Fig. 6A4) in the Dox group while normal morphology of cardiac myocytes was observed in control (Fig. 6A1) and Chi/DPo3–Dox (Fig. 6A2) groups. Similarly, mice treated with free Dox

exhibited epidermal necrosis (Fig. 6B4) and vacuolization (Fig. 6B5 and B6) while the morphology of skin from Chi/DPO3–Dox group was not perturbed (Fig. 6B3), and similar to the samples from control (Fig. 6B1) and Chi/DPO3 (Fig. 6B2) groups.

4. Discussion

In the previous study, we have demonstrated the thermosensitive, pH-dependent, and sustained releasing properties of Chi/DPO hydrogels which are liquid at low or room temperature but gel at body temperature (37 °C) [26]. In this study, various Chi/DPO formulations were prepared and characterized to determine the suitable formulation for the release of Dox, a frontline chemotherapeutic agent. Due to different combinations, various gelation properties were recorded for these formulations. All of them had gelation temperature above room temperature, ranging from 22 to 30.3 °C. At room temperature, they started the gelation process after 1–7.1 min. All of them gelled immediately at 37 °C. The G′ of these hydrogels varied from 258.7 Pa to 2701 Pa. Their pH values ranged from 7.20 to 7.54 which are within the acceptable pH range for injectable pharmaceutical products.

Chi/DPO1 appeared as the weakest hydrogel but it was the most stable formulation at room temperature, demonstrated by its longest gelation time at this temperature (7.1 min). Chi/DPO4 produced the strongest hydrogel but it started to gel at relatively low temperature, 22 °C which was very close to room temperature. It was also the least stable formulation at room temperature since it remained in liquid state for only 1 min. Chi/DPO2, Chi/DPO3, and Chi/DPO5 exhibited rheological properties acceptable for injectable drug delivery system.

The effect of Dox on the gelation behavior of Chi/DPO was also investigated. Dox was found to slightly influence the gelation temperature and gelation time of the Chi/DPO solutions (data not shown). Generally in the presence of Dox, Chi/DPO gelled at a lower temperature and their gelation time was a bit shorter.

The release of Dox was controlled and governed by the hydrogel combinations. Interestingly, the release patterns of Dox from Chi/DPO formulations were not influenced by chitosan concentration and the hydrogel strength. They were factors affecting the release of proteins entrapped in Chi/DPO hydrogels as presented in our previous study [26]. The amount of orthophosphate salt in formulations was the key factor significantly influencing Dox release profiles, especially the initial burst effect. After 1 day of study, Chi/DPO5, the formulation containing the smallest amount of salt, released the highest percentage of entrapped Dox (27.5%) despite its high gel strength (1238 Pa) compared to other formulations. Although Chi/DPO2 and Chi/DPO4 had different chitosan concentrations (2.5% and 2.9%) and their gel strength exhibited a large gap (549.3 and 2701 Pa), they produced the same release patterns with equal initial burst effects (29% after 1 day). This might be due to the same amount of salt present in these formulations. Similarly, despite the different compositions and the rheological properties of Chi/DPO1 and Chi/DPO3, these hydrogels released Dox in the same patterns. Within 1 day of the experiment, approximately 19% of the loaded Dox diffused out of these gel matrices. These formulations also had relatively equivalent amounts of salt.

These results can be explained by the morphology of Chi/DPO hydrogels. We found that the larger outer pores were formed in the formulations containing less orthophosphate (data not shown), which could lead to the higher initial burst release of small molecules such as Dox (Mw: 578 Da) from these formulations. It was noted that after the initial burst in day 1, the cumulative release percentages of Dox from five formulations did not differ much from each other (around 8.5–10.5%). It indicated that the composition of
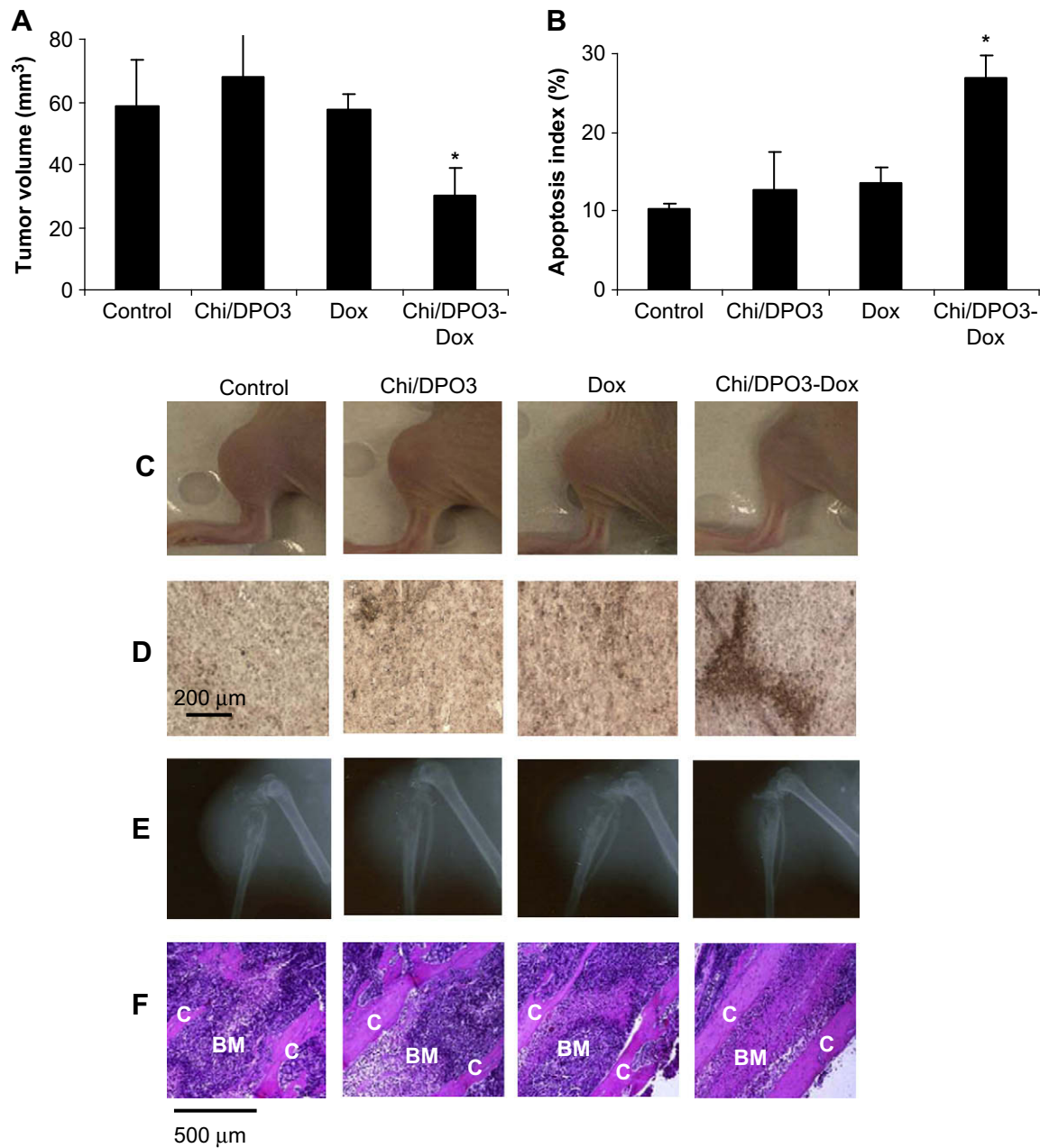
Fig. 4. Inhibitory effect of Chi/DPO3–Dox on *in vivo* tumor growth in mice after 12 days post-treatment. (A) Tumor growth inhibition graph, *$P < 0.05$ vs. control group. (B) Tumor apoptosis graph, *$P < 0.05$ vs. control group. (C) Primary tumors, showing significantly large tumors in samples from control, Chi/DPO3 and Dox groups, but nearly nil tumors in sample from Chi/DPO3–Dox group. (D) TUNEL-stained apoptotic tumor tissues, showing much less apoptotic cells (dark brown) in tumor tissues from control, Chi/DPO3 and Dox groups, compared to tumor tissue from Chi/DPO3–Dox group (magnification ×40). (E) X-ray images, indicating severe bone lysis in samples from control, Chi/DPO3 and Dox groups and only mild osteolysis observed in sample from Chi/DPO3–Dox group. (F) Histological analysis of tumor growth, showing that tumor cells severely degraded bone cortex and invaded bone marrow in samples from control, Chi/DPO3 and Dox groups, with less bone degradation in sample from Chi/DPO3–Dox group (BM: bone marrow, C: cortex) (magnification ×200).

Chi/DPO hydrogel did not dramatically affect the release pattern of small molecules during linear phase. However, the amount of salt contributed in the hydrogel significantly influenced the initial burst effect. Therefore, by varying the salt amount, the degree of the burst release of small molecules could be adjusted.

The release profile of Dox from Chi/DPO3 hydrogels was also affected by the load of Dox in the formulations. It was found that the higher-loaded formulation (2.5 mg/ml) showed a higher initial burst and a greater release rate during linear stage (in terms of mass amount). In BALB/c mice, the LD50 (the drug doses that results in death of one-half of the tested animals) value for Dox administered

intraperitoneal injection was 20.6 mg Dox/kg body weight [27]. Therefore, in the *in vivo* efficacy study, a dose of 5 mg Dox/kg mouse body weight was chosen to treat mice. Since each mouse had average weight of 20 g, it needed a total of 100 μg Dox. Although the initial burst of the formulation containing 2.5 mg/ml Chi/DPO3 was higher, it was within the acceptable limit. On the other hand, this formulation provided more sustained release of Dox, compared to the lower-loaded formulation (Fig. 1C). In addition, higher load can reduce the volume of Chi/DPO solution injected, leading to better patience compliance. Therefore, the higher-loaded formulation was selected for later experiments.
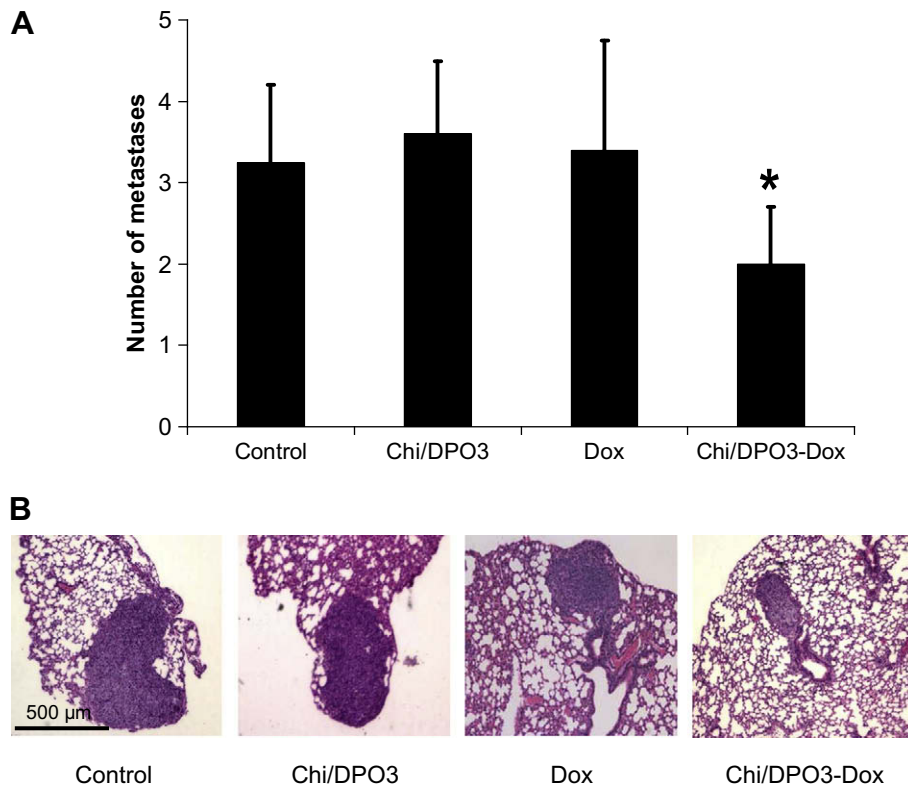
Fig. 5. Inhibition of lung macrometastasis in mice after 12 days post-treatment. (A) Lung macrometastasis inhibition graph, $^*P < 0.05$ vs. control group. The number of macrometastases was enumerated on the surface of all lobes of each lung against a white background. (B) Histological analysis of lung metastasis (P: parenchyma, T: tumor) (magnification ×40).

It was noticed that after the initial burst, the release rate of Dox was slow and seemed to reach plateau within a short time frame. It may raise doubts on the sustained release property of Chi/DPO hydrogels. However, in in vivo conditions, it is expected that the release rate of the entrapped agents would be higher due to the degradation of the chitosan network caused by various enzymes and macrophages present in the body. To prove it, lysozyme was added to the release media at a concentration of 8 µg/ml (similar to the enzyme concentration found in human serum [28]). Chitosan is known to be degraded or metabolized in vivo by certain enzymes, especially lysozyme through the hydrolysis of the acetylated residues [29]. The rate of this degradation inversely depends on the degree of acetylation and crystallinity of the polymer. As expected, in the presence of the enzyme, the initial burst increased by approximately 2% and the release rate after the initial burst increased by 6 times. In addition, the release was well sustained over the period of 19 days. These results confirm the ability of Chi/DPO hydrogels in controlling and sustaining the release of Dox.

The viability of SaOS-2 cells in the presence of Chi/DPO3–Dox is presented in Fig. 2A in comparison with the cell viability in culture containing blank Chi/DPO3 or free Dox. Different numbers of cells were employed. It was found that Chi/DPO3 did not cause any significant effect on the viability of SaOS-2 cells, indicating the biocompatibility of this hydrogel formulation. It appeared that free Dox had more potent activity than Chi/DPO3–Dox, especially in the presence of a higher number of cells. These results can be explained by a sustained release property of Dox from Chi/DPO3 hydrogel matrix.

Dox belongs to the anthracyclines antibiotics, and its anti-tumor activity is related to the ability of binding DNA and inhibition of nucleic acid synthesis, leading to the apoptosis of tumor cells [30]. Apoptosis is a form of programmed cell death in multicellular organisms [31,32], which involves a series of biochemical events leading to a variety of morphological changes and death of cells [33,34]. As can be seen in Fig. 3, Chi/DPO3–Dox induced approximately 85% of total cells to be apoptotic while Chi/DPO3 did not. It again demonstrated the biocompatibility of Chi/DPO3 and the activity of Dox released from the hydrogel matrix.

The local delivery of Dox from the formulation injected peritumorally and its anti-tumor activity were demonstrated via the investigation of tumor growth. Fig. 4 reveals the ability of Chi/DPO3–Dox to inhibit primary tumor growth at the tibial site. It shows a significant difference between tumor growth in the control group and the Chi/DPO3–Dox injected group. Chi/DPO3–Dox reduced the tumor volumes by approximately 50% compared to untreated (control) group. However, the same did not hold for the Chi/DPO3-injected and free Dox-injected groups, which did not demonstrate any growth inhibition. Over the 12 days of experiment, the control tumors were 58.44 ± 14.93 mm^3 in size and the free Dox-injected tumors had size at 57.36 ± 4.85 mm^3 while the Chi/DPO3–Dox treated tumors were only 30.26 ± 8.74 mm^3. The difference was statistically significant ($P < 0.05$) between the Chi/DPO3–Dox group and both the control and the free Dox groups. Both X-ray and histology analysis revealed lesser evidence of bone degradation (osteolysis) in the groups of Chi/DPO3–Dox. These results indicate that Chi/DPO3–Dox treatment had significantly better ability to delay tumor growth, compared to the free Dox treatment with the same Dox dose.

Chitosan is a biomaterial which has been used for bone generation [35], probably through its stimulatory effects on periodontal ligament fibroblasts and its ability to enhance type I collagen
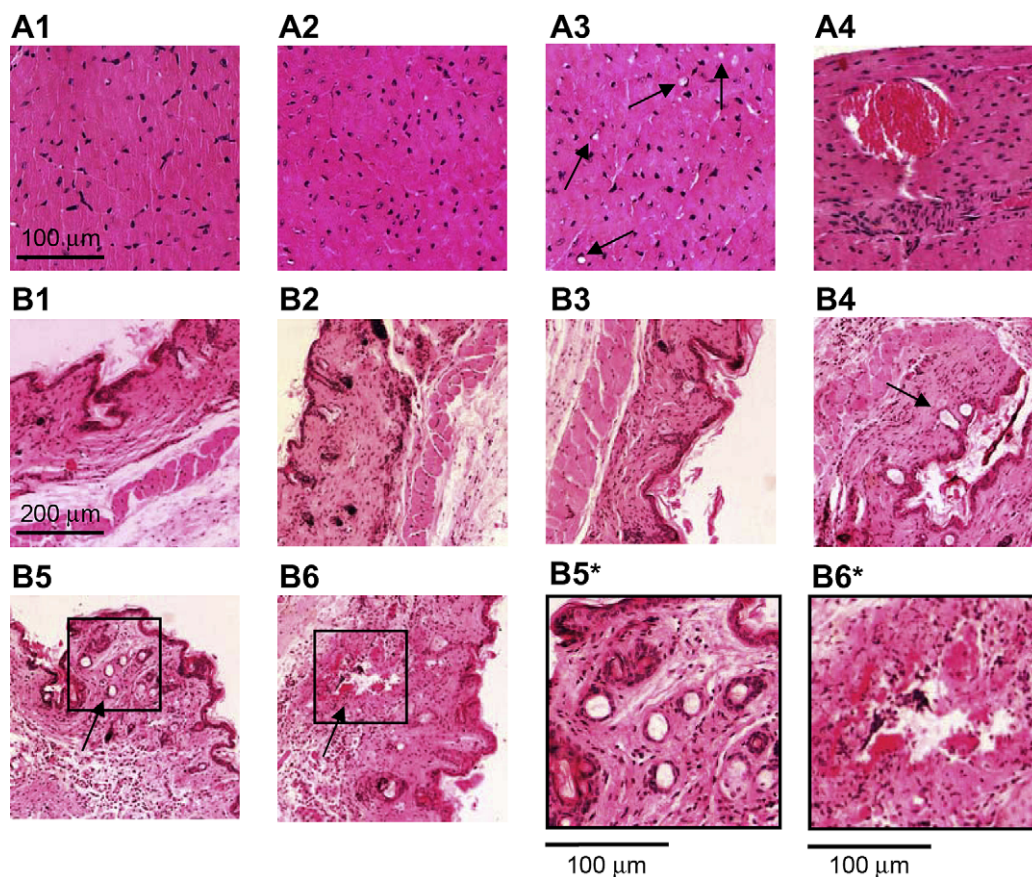
Fig. 6. Reduction of systemic side-effects of Dox after 12 days post-treatment. (A) Histological analysis of heart sections (magnification ×200). Cardiac tissue from control group (A1) and cardiac tissue in mice peritumorally injected with Chi/DPO3–Dox (A2) showing normal morphology. Cardiac tissue from mice intraperitoneally injected with free Dox showing myocytes with cytoplasmic vacuolization (A3) and vascular dilation (A4) (black arrows). (B) Skin sections of nude mice (magnification ×100). Skin sections from control group (B1), Chi/DPO3-injected mice (B2), mice peritumorally injected with Chi/DPO3–Dox (B3) showing normal morphology. Mice intraperitoneally injected with free Dox showing epidermal vacuolization (B4 and B5) and epidermal necrosis (B6) (black arrows). (B5* and B6*) representing exploded views of B5 and B6, respectively.

(major type of protein in bone) synthesis [36]. It was found that there was no inflammatory response to the use of chitosan *in vivo* in both mouse and rabbit species [35]. The results from this study also demonstrated the biocompatibility of the Chi/DPO hydrogel system in mice.

Lungs are the predominant site for OS metastasis, and in quite a number of cases, is life-threatening [1,23]. Despite the aggressive treatment, 1 in 3 patients still develop pulmonary metastases, and this remains the major cause of death from this condition [4,37]. SaOS-2 metastases were mostly extravascular and growing within the parenchyma and randomly in shape [3]. In this study, the inhibition effect of Chi/DPO3–Dox on lung metastases was also investigated. The obtained results indicate that Chi/DPO3–Dox treatment had significantly better ability to delay metastasis growth, compared to the free Dox treatment with the same Dox dose.

Doxorubicin (Dox) or hydroxyldaunorubicin is a widely used chemotherapeutic drug for various cancers such as tumors of brain [38], breast [39], ovaries, lung, prostate, cervix, bladder [40], and bone [8]. Dox is a 14-hydroxylated version of daunorubicin, the immediate precursor of Dox in its biosynthetic pathway. It works by interfering with the growth of rapidly growing cancer cells where it binds and intercalates into the DNA strand, thus inhibiting further DNA and RNA biosynthesis, eventually causing cell death [41–43]. In spite of its potent anti-cancer activity, the nonspecific action of Dox causes serious side-effects to the patients such as heart and skin complications [7,40]. It can also cause neutropenia (a decrease

in white blood cells), as well as complete alopecia (hair loss). Dox side-effects remain a common clinical problem. In this study, it was found that the controlled and sustained release of Dox via Chi/DPO3 considerably reduced Dox side-effects in mice including cardiotoxicity (Fig. 6A) and skin toxicity (Fig. 6B). Like many other drugs used to treat cancer, Dox is a potent vesicant that may cause extravasations and necrosis at the injection site or any site that the skin is exposed to [40]. It this study, no necrosis was observed in mice skin at the injection site and other sites as well. These results indicate that the Chi/DPO3–Dox treatment had significantly better ability to reduce systemic side-effects, compared to the free Dox treatment with the same Dox dose.

The above results can be explained by the localized and sustained release of Dox from Chi/DPO hydrogel, leading to the prolonged and continuous direct actions of Dox on cancerous cells. Since only small amount of Dox was released at a specific time point within the local site, the possibility of Dox travelling to other organs and causing side-effects was minimized. In contrast, the conventional administration of Dox via intraperitoneal injection allowed Dox to go through every organ, thus the probability of systemic side-effects is high. Furthermore, as only a small portion of injected dose could reach the targeted tumor, it had limited inhibition effect on the growth of tumor. In addition, since it provided a sudden high amount of Dox in a short time period which then dropped quickly, there was no prolonged anti-tumor activity presented in this treatment and the need of repeated doses was crucial.

5. Conclusion

The potential application of the Chi/DPO hydrogel drug delivery system (DDS) for OS treatment has been demonstrated in a clinically relevant orthotopic and metastatic mouse model. Doxorubicin, an anti-tumor agent was successfully released from this DDS in a sustained manner with its function preserved. The incorporation of Dox in Chi/DPO not only significantly inhibited the growth of OS, osteolysis and lung metastasis, but also reduced the side-effects of Dox in mice, compared to the conventional administration of Dox. The biocompatibility of Chi/DPO system was also demonstrated through this study. These results highlight the promising application of chitosan/orthophosphate hydrogel as an effective DDS for a successful chemotherapy.

Acknowledgement

Appendix

Figures with essential colour discrimination. Parts of the majority of figures in this article are difficult to interpret in black and white. The full colour images can be found in the on-line version, at doi:10.1016/j.biomaterials.2009.03.022.

References

[1] Longhi A, Errani C, De Paolis M, Mercuri M, Bacci G. Primary bone osteosarcoma in the pediatric age: state of the art. Cancer Treat Rev 2006;32:423–36.
[2] Quan GMY, Ojaimi J, Nadesapillai WAP, Zhou H, Choong PFM. Resistance of epiphyseal cartilage to invasion by osteosarcoma of antiangiogenic factors. Pathobiology 2002;70:361–7.
[3] Dass CR, Ek ET, Contreras KG, Choong PF. A novel orthotopic murine model provides insights into cellular and molecular characteristics contributing to human osteosarcoma. Clin Exp Metastasis 2006;23:367–80.
[4] Ferrari S, Smeland S, Mercuri M, Bertoni F, Longhi A, Ruggieri P, et al. Neoadjuvant chemotherapy with high-dose ifosfamide, high-dose methotrexate, cisplatin and doxorubicin for patients with localized osteosarcoma of the extremity: a joint study by the Italian and Scandinavian Sarcoma Groups. J Clin Oncol 2005;23:8845–52.
[5] Ferguson WS, Goorin AM. Current treatment of osteosarcoma. Canc Invest 2001;19:292–315.
[6] Patel SJ, Lynch JWJ, Johnson T, Carroll RR, Schumacher CRN, Spanier S, et al. Dose-intense ifosfamide/doxorubicin/cisplatin based chemotherapy for osteosarcoma in adults. Am J Clin Oncol 2002;25:489–95.
[7] Sadea W, Torti FM. Principles of pharmacology and cancer chemotherapy. In: Ellmann K, Carter SK, editors. Fundamentals of cancer chemotherapy. New York: McGraw-Hill; 1987. p. 19–27.
[8] Fan H, Dash AK. Effect of cross-linking on the in vitro release kinetics of doxorubicin from gelatin implants. Int J Pharm 2001;213:103–16.
[9] Cohen JL, Chan KK. Pharmacokinetics and distribution studies with adriamycin. In: Weiss L, Gillbert HA, editors. Bone metastasis. Boston, MA: Hall Medical Publishers; 1981. p. 276–99.
[10] Gabizon A, Martin F. Polyethylene glycol-coated (pegylated) liposomal doxorubicin. Drugs 1997;54:15–21.
[11] Lasic DD. Doxorubicin in sterically stabilized liposomes. Nature 1996;380:561–2.
[12] Stolnik S, Illum L, Davis SS. Long circulation microparticulate drug carriers. Adv Drug Deliv Rev 1995;16:195–214.
[13] Rolland S, O'Mullane J, Goddard P, Brookman L, Petrak K. New macromolecular carriers for drugs. I. Preparation and characterization of poly(oxyethylene-b-isoprene-b-oxyethylene) block copolymer aggregates. J Appl Polym Sci 1992;44:1195–203.
[14] Kwon GS, Suwa S, Yokoyama M, Okano T, Sakurai S, Kataoka K. Enhanced tumor accumulation and prolonged circulation times of micelle-forming poly(ethylene oxide-co-aspartate) block copolymer-adriamycin conjugates. J Control Release 1994;29:17–23.
[15] Dvorak M, Kopeckova P, Kopecek J. High-molecular weight HPMA copolymer-adrimycin conjugates. J Control Release 1999;60:321–32.
[16] Kubo T, Sugita T, Shimose S, Nitta Y, Ikuta Y, Murakami T. Targeted systemic chemotherapy using magnetic liposomes with incorporated adriamycin for osteosarcoma in hamsters. Int J Oncol 2001;18:121–5.
[17] Itokazu M, Kumazawa S, Wada E, Wenyi Y. Sustained release of adriamycin from implanted hydroxyapatite blocks for the treatment of experimental osteogenic sarcoma in mice. Cancer Lett 1996;107:11–8.
[18] Fisher JL, Mackie PS, Howard ML, Zhou H, Choong PFM. The expression of the urokinase plasminogen activator system in metastatic murine osteosarcoma: an in vivo mouse model. Clin Cancer Res 2001;7:1654–60.
[19] Winter HH, Chambon F. Analysis of linear viscoelasticity of crosslinking polymer at gel point. J Rheol 1986;30:367–82.
[20] Chenite A, Gori S, Chive M, Desrosiers E, Buschmann MD. Monolithic gelation of chitosan solutions via enzymatic hydrolysis of urea. Carbohydr Polym 2006;64:419–24.
[21] Cho J, Heuzey M-C, Begin A, Carreau PJ. Effect of urea on solution behaviour and heat-induced gelation of chitosan-b-glycerophosphate. Carbohydr Polym 2006;63:507–18.
[22] Berlin O, Samid D, Donthineni-Rao R, Akeson W, Amiel D, Woods VL. Development of a novel spontaneous metastasis model of human osteosarcoma transplanted orthotopically into bone of athymic mice. Cancer Res 1993;53:4890–5.
[23] Dass CR, Contreras KG, Dunstan DE, Choong PFM. Chitosan microparticles encapsulating PEDF plasmid demonstrate efficacy in an orthotopic metastatic model of osteosarcoma. Biomaterials 2007;28:3026–33.
[24] Ek ETH, Dass CR, Contreras KG, Choong PFM. Pigment epithelium-derived factor overexpression inhibits orthotopic osteosarcoma growth, angiogenesis and metastasis. Cancer Gene Ther 2007;14:616–26.
[25] Rawlins EA. Diffusion. Bentley's textbook of pharmaceutics. 8th ed. London: Tindall and Cox; 1984 [chapter 8].
[26] Ta HT, Han H, Larson I, Dass CR, Dunstan DE. Chitosan-dibasic orthophosphate hydrogel: a potential drug delivery system. International Journal of Pharmaceutics 2009. doi:10.1016/j.ijpharm.2009.01.018.
[27] Wong HL, Rauth AM, Bendayan R, Wu XY. In vivo evaluation of a new polymer-lipid hybrid nanoparticles (PLN) formulation of doxorubicin in a murine solid tumor model. Eur J Pharm Biopharm 2007;65:300–8.
[28] Montagne P, Cuiliere ML, Mole C, Bene MC, Faure G. Microparticle-enhanced nephelometric immunoassay of lysozyme in milk and other human body fluids. Clin Chem 1998;44:1610–5.
[29] Tomihata K, Ikada Y. In vitro and in vivo degradation of films of chitin and its deacetylated derivatives. Biomaterials 1997;18:567–75.
[30] Gerwirtz DA. A critical evaluation of the mechanism of action proposed for the antitumor effects of the anthracycline antibiotics adriamycin and daunorubicin. Biochem Pharmacol 1999;57:727–41.
[31] Ellis RE, Yuan JY, Horvitz HR. Mechanisms and functions of cell death. Ann Rev Cell Biol 1991;7:663–98.
[32] Steller H. Mechanisms of genes of cellular suicide. Science 1995;267:1445–9.
[33] Kerr JF. A histochemical study of hypertrophy and ischaemic injury of rat liver with special reference to changes in lysosomes. J Pathol Bacteriol 1965;90:419–35.
[34] Kerr JF, Wyllie AH, Currie AR. Apoptosis: a basic biological phenomenon with wide-ranging implications in tissue kinetics. Br J Cancer 1972;26:239–57.
[35] Shin YH, Park HN, Kim KH, Lee MH, Lee MH, Choi YS, et al. Biological evaluation of chitosan nanofiber membrane for guided bone generation. J Periodontol 2005;76:1778–84.
[36] Pang EK, Paik JW, Kim SK, Jung UW, Kim CH, Cho KS. Effects of chitosan on human periodontal ligament fibroblasts in vitro and on bone formation in rat calvarial defects. J Periodontol 2005;76:1526–33.
[37] Petrilli AS, de Camargo B, Filho VO, Bruniera P, Brunetto AL, Jesus-Garcia R, et al. Results of the Brazilian osteosarcoma treatment group Studies III and IV: prognostic factors and impact on survival. J Clin Oncol 2006;24:1161–8.
[38] Lesniak MS, Upadhyay U, Goodwin R, Tyler B, Brem H. Local delivery of doxorubicin for the treatment of malignant brain tumors in rats. Anticancer Res 2005;25:3825–31.
[39] Wong HL, Bendayan R, Rauth AM, Wu XY. Simultaneous delivery of doxorubicin and GG918 (elacridar) by new polymer–lipid hybrid nanoparticles (PLN) for enhanced treatment of multidrug-resistant breast cancer. J Control Release 2006;116:275–84.
[40] Lin R, Ng LS, Wang C-H. In vitro study of anticancer drug doxorubicin in PLGA-based microparticles. Biomaterials 2005;26:4476–85.
[41] Di Marco A. Adriamycin (NSC-123127): mode and mechanism of action. Cancer Chemother Rep 1975;6:91–106.
[42] Goodman MF, Lee GM, Bachur NR. Adriamycin interactions with T4 DNA polymerase. J Biol Chem 1977;252:2670–4.
[43] Schwartz HS. DNA breaks in P-288 tumor cells in mice after treatment with daunorubicin and adriamycin. Res Commun Chem Pathol Pharmacol 1975;10:51–64.